Int. J. Therm. Sci. (2000) 39, 605–615

S1290-0729(00)00209-X/FLA

Effects of heat absorption and thermal radiation on heat transfer in a fluid–particle flow past a surface in the presence of a gravity field

Ali J. Chamkha

Department of Mechanical and Industrial Engineering, Kuwait University, P.O. Box 5969, Safat, 13060, Kuwait

(Received 7 June 1999, accepted 9 October 1999)

Abstract — A continuum two-phase fluid–particle model accounting for fluid-phase heat generation or absorption and thermal radiation is developed and applied to the problem of heat transfer in a particulate suspension flow over a horizontal heated surface in the presence of a gravity field. Analytical solutions for the temperature distributions and the wall heat fluxes for both phases are obtained. Two cases of wall thermal conditions corresponding to stationary and periodic temperature distributions are considered. Numerical evaluations of the analytical solutions are performed and the results are reported graphically to elucidate special features of the solutions. The effects of heat absorption and thermal radiation are illustrated through representative results for the temperature distributions and heat fluxes of both phases for various fluid–particle suspensions. It is found that heat absorption increases the total heat transfer rate for various particulate volume fraction levels while thermal radiation decreases it. © 2000 Éditions scientifiques et médicales Elsevier SAS

Nomenclature

a	particle radius	m
c	fluid-phase specific heat at constant pressure	$J{\cdot}kg^{-1}{\cdot}K^{-1}$
Ec	Eckert number $= (ga^2\gamma/\nu)^2/(c(T_w - T_\infty))$	
f	correction factor defined by equation (9)	
g	gravitational acceleration	$m{\cdot}s^{-2}$
k	specific heat ratio $k = c_p/c$	
K	mean radiation absorption coefficient	
N	dimensionless thermal radiation coefficient $= 16\sigma T_\infty^3/(K\lambda_c)$	
p	fluid-phase pressure	Pa
P	dimensionless fluid-phase pressure	
Pr	Prandtl number $= \nu/\kappa$	
q_f	fluid-phase convective heat transfer rate defined by equation (50)	$W{\cdot}m^{-2}$
q_p	particle-phase sensible heat transfer rate defined by equation (51)	$W{\cdot}m^{-2}$
q_r	radiative heat flux defined by equation (10)	$W{\cdot}m^{-2}$
q_T	total heat transfer rate $= q_f + q_p$	$W{\cdot}m^{-2}$
Q_f	dimensionless fluid-phase convective heat transfer rate	
Q_p	dimensionless particle-phase sensible heat transfer rate	
Q_T	dimensionless heat transfer rate $= q_T a/(\kappa\rho c(T_w - T_\infty))$	
Q_0	heat generation or absorption coefficient	W
Re	Reynolds number $= ga^3\gamma/\nu^2$	
t	time	s
T	fluid-phase temperature	K
u	fluid-phase x-component of velocity	$m{\cdot}s^{-1}$
U	dimensionless fluid-phase x-component of velocity $= \nu/(ga^2\gamma)u$	
v	fluid-phase y-component of velocity	$m{\cdot}s^{-1}$
V	dimensionless fluid-phase y-component of velocity $= \nu/(ga^2\gamma)v$	
x	distance along the surface	m
y	distance normal to the surface	m

Greek symbols

α	volume fraction of particles
α_m	dense sediment particulate volume fraction ($\alpha_m \approx 0.6$)
η	dimensionless vertical distance $= y/a$
γ	particle loading $= \rho_p/\rho$

chamkha@kuc01.kuniv.edu.kw

κ	fluid-phase thermal diffusivity $= \lambda_c/(\rho c)$	$m^2 \cdot s^{-1}$
λ_c	fluid-phase thermal conductivity	$W \cdot m^{-1} \cdot K^{-1}$
μ	fluid-phase dynamic viscosity	Pa·s
ν	fluid-phase kinematic viscosity	$m^2 \cdot s^{-1}$
ω	frequency of oscillation of wall temperature	s^{-1}
ϕ	dimensionless heat generation or absorption coefficient $= Q_0 a^2/(3\lambda_c)$	
ρ	fluid-phase density	$kg \cdot m^{-3}$
σ	Stefan–Boltzmann constant	$W \cdot m^{-2} \cdot K^{-4}$
τ	dimensionless time $= ga\gamma/\nu t$	
θ	dimensionless fluid-phase temperature $= (T - T_\infty)/(T_w - T_\infty)$	
ξ	a constant to apportion heat dissipation between the phases	

Subscripts

i	interface
p	particle phase
w	wall
∞	free stream

1. INTRODUCTION

The process of particulate deposition from flowing fluid/solid suspensions and the consequent heat transfer characteristics are important in various natural and engineering applications. Some possible applications include deep-bed and membrane filtration, fouling of heat transfer surfaces, atmospheric pollution and microbial and cell transport in living systems (Yiantsios and Karabelas [1]). There have been considerable research work done on particulate deposition in laminar flows such as the reviews by Jia and Williams [2] and van de Ven [3]. Sedimentation effects for particle sizes close to one micron or larger are reported by Yao et al. [4]. Adamczyk and van de Ven [5, 6] have considered particulate deposition in rectilinear flows over flat surfaces. Marmur and Ruckenstein [7] have reported on the process of cells deposition on a flat plate. Apazidis [8, 9] has analyzed the velocity and temperature distributions of two-dimensional laminar flows of a particulate suspension in the presence of a gravity field. More recently, Dahlkid [10] has considered the motion of Brownian particles and sediment on an inclined plate. This work was done in relation to the process of separation of proteins, viruses, antibodies, and vaccines. Yiantsios and Karabelas [1] has studied the effect of gravity on the deposition of micron-sized particles on smooth surfaces. Their work was focused on particulate deposition from liquid suspensions with the main motivation being fouling of heat transfer or filtration equipment by suspended particles.

In many fluid–particle flows, the fluid heat generation or absorption and the thermal radiation effects may play an important role in altering the heat transfer characteristics. Vajravelu and Nayfeh [11] and Vajravelu and Hadjinicolaou [12] have considered the effects of temperature-dependent heat generation or absorption on heat transfer in different geometries. Thermal radiation effects on flow of micropolar fluids past a continuously moving plate has been considered by Raptis [13]. Also, Raptis [14] has analyzed thermal radiation and free convection flow through a porous medium. Thermal radiation effects in particulate suspensions are especially important in multiphase systems consisting of solid particulates and gases. The role of thermal radiation in these systems is of major importance in the design of fluidized beds, packed beds, catalytic reactors and many other advanced energy conversion systems operating at high temperatures (Tien and Vafai [15]). Thermal radiation within these systems is usually the result of emission by the hot walls and the gas–particle mixture. This radiation undergoes complex interaction with the system, primary due to absorption and scattering processes. Examples of previous studies of radiative heat transfer through porous beds can be found in the works of Vortmeyer [16] and Tien [17].

In the present work, a very simple two-phase model is employed in which the suspension is assumed to be dilute in the sense that no interparticle collision exist and that the thermal radiation is absorbed by the fluid and the energy is then transferred to the particle phase through the interphase heat transfer mechanism. The fluid phase is considered to be a gray, absorbing and emitting radiation but the particles are assumed to be nonscattering and that the Rosseland approximation is employed to describe the radiative heat flux in the fluid-phase energy equation. The particle phase is assumed to have uniform density distribution and is made of spherical particles having one size. The present work is a direct generalization of the work reported by Apazidis [9] on the heat transfer characteristics of particle–fluid flow past a heated infinite horizontal plate.

2. GOVERNING EQUATIONS

Consider unsteady laminar flow of a two-phase particulate suspension over a heated horizontal infinite surface maintained at a constant temperature T_w in the presence of a gravity field, heat generation or absorption and thermal radiation. The surface is coincident with the half plane $y = 0$, $x \geq 0$ and the flow far from the surface is

a uniform stream in the x-direction parallel to the surface with both phases being in both hydrodynamic and thermal equilibrium. Due to the density difference between both the fluid and particle phases, a separational motion in which heavy particles falling from the flow form a layer of dense sediment on the surface while the carrier fluid flows in the opposite upward direction is introduced. This settling process is called sedimentation (Wallis [18]). According to Kynch [19] and later by Apazidis [8], the vertical sedimentation of solid particles may proceed in three different ways, depending on the shape of the curve of the total particle flow rate versus the volume fraction of particles in the mixture. Apazidis [8] has considered the case when a direct shock from the initial value of the particulate volume fraction α to the final fully settled value α_{M} is formed at the interface of the mixture and the settled particles with maximum packing at the surface. The particle phase is assumed to be made up of spherical solid particles having one size and with a uniform density distribution. The particle Reynolds number is assumed to be less than unity so that the force interaction between the phases is limited to the Stokes drag. Based on the above assumptions and treating the particle phase as a continuum (Marble [20]), the governing equations for this investigation can be written as

$$-\frac{\partial \alpha}{\partial t}+\frac{\partial}{\partial y}\big((1-\alpha)v\big)=0 \tag{1}$$

$$(1-\alpha)\rho\left(\frac{\partial u}{\partial t}+v\,\frac{\partial u}{\partial y}\right)=(1-\alpha)\mu\,\frac{\partial^2 u}{\partial y^2}-\frac{9}{2}\,f(\alpha)\frac{\mu}{a^2}(u-u_{\mathrm{p}}) \tag{2}$$

$$(1-\alpha)\rho\left(\frac{\partial v}{\partial t}+v\,\frac{\partial v}{\partial y}\right)=(1-\alpha)\left(\mu\,\frac{\partial^2 v}{\partial y^2}-\frac{\partial p}{\partial y}-\rho g\right)-\frac{9}{2}\,f(\alpha)\frac{\mu}{a^2}(v-v_{\mathrm{p}}) \tag{3}$$

$$(1-\alpha)\rho c\left(\frac{\partial T}{\partial t}+v\,\frac{\partial T}{\partial y}\right)=(1-\alpha)\lambda_{\mathrm{c}}\,\frac{\partial^2 T}{\partial y^2}-3\frac{\lambda_{\mathrm{c}}\alpha}{a^2}(T-T_{\mathrm{p}})+(1-\alpha)Q_0(T-T_\infty)-(1-\alpha)\frac{\partial q_{\mathrm{r}}}{\partial y} \tag{4}$$

for the fluid phase and

$$\frac{\partial \alpha}{\partial t}+\frac{\partial}{\partial y}(\alpha v_{\mathrm{p}})=0 \tag{5}$$

$$\alpha\rho_{\mathrm{p}}\left(\frac{\partial u_{\mathrm{p}}}{\partial t}+v_{\mathrm{p}}\,\frac{\partial u_{\mathrm{p}}}{\partial y}\right)=\frac{9}{2}\,f(\alpha)\frac{\mu}{a^2}(u-u_{\mathrm{p}}) \tag{6}$$

$$\alpha\rho_{\mathrm{p}}\left(\frac{\partial v_{\mathrm{p}}}{\partial t}+v_{\mathrm{p}}\,\frac{\partial v_{\mathrm{p}}}{\partial y}\right)=\alpha\left(-\frac{\partial p}{\partial y}-\rho_{\mathrm{p}}g\right)+\frac{9}{2}\,f(\alpha)\frac{\mu}{a^2}(v-v_{\mathrm{p}}) \tag{7}$$

$$\alpha\rho_{\mathrm{p}}c_{\mathrm{p}}\left(\frac{\partial T_{\mathrm{p}}}{\partial t}+v_{\mathrm{p}}\,\frac{\partial T_{\mathrm{p}}}{\partial y}\right)=3\frac{\lambda_{\mathrm{c}}}{a^2}\alpha(T-T_{\mathrm{p}}) \tag{8}$$

for the particle phase. Here t is time and y is the vertical distance. u, v, p and T are the fluid-phase x-component of velocity, y-component of velocity, pressure, and temperature, respectively. α, ρ, μ, λ_{c}, and c are the volume fraction of particles and the fluid-phase density, dynamic viscosity, thermal conductivity, and specific heat, respectively. a, g, Q_0, q_{r} and T_∞ are the particle radius, gravitational acceleration, heat generation or absorption coefficient, radiative heat flux and the free stream temperature. A subscript p indicates particle phase. It should be noted that positive values of Q_0 indicate heat generation while negative values of Q_0 correspond to heat absorption conditions.

Equations (1)–(8) are supplemented by the function $f(\alpha)$ which is reported by Tam [21] and employed by Apazidis [8, 9] such that

$$f(\alpha)=\frac{\alpha(4+3(8\alpha-3\alpha^2)^{1/2}+3\alpha)}{(2-3\alpha)^2} \tag{9}$$

It should be mentioned that $f(\alpha)$ represents a correction factor for the Stokes drag force on a single spherical particle which accounts for finite volume fraction of the particle phase.

In addition, the radiative heat flux q_{r} is employed according to Rosseland approximation such that

$$q_{\mathrm{r}}=-\frac{4\sigma}{3K}\,\frac{\partial T^4}{\partial y} \tag{10}$$

where σ and K are the Stefan–Boltzmann constant and the mean absorption coefficient, respectively. As done by Raptis [13, 14], the fluid-phase temperature differences within the flow are assumed to be sufficiently small so that T^4 may be expressed as a linear function of temperature. This is done by expanding T^4 in a Taylor series about the free stream temperature T_∞ and neglecting higher-order terms to yield

$$T^4=4T_\infty^3T-3T_\infty^4 \tag{11}$$

By using equations (10) and (11) in the last term of equation (4) one obtains

$$\frac{\partial q_{\mathrm{r}}}{\partial y}=-\frac{16\sigma T_\infty^3}{3K}\,\frac{\partial^2 T}{\partial y^2} \tag{12}$$

It is convenient to nondimensionalize the above governing equations by using

$$\begin{aligned}
&\eta = \frac{y}{a}, && \tau = \frac{ga\gamma}{\nu}t, && u = \frac{ga^2\gamma}{\nu}U \\
&u_{\mathrm{p}} = \frac{ga^2\gamma}{\nu}U_{\mathrm{p}}, && v = \frac{ga^2\gamma}{\nu}V, && v_{\mathrm{p}} = \frac{ga^2\gamma}{\nu}V_{\mathrm{p}} \\
&\theta = \frac{T-T_\infty}{T_{\mathrm{w}}-T_\infty}, && \theta_{\mathrm{p}} = \frac{T_{\mathrm{p}}-T_\infty}{T_{\mathrm{w}}-T_\infty} && \\
&p = -\rho g y(1-\gamma P) &&&&
\end{aligned} \tag{13}$$

to yield

$$-\frac{\partial\alpha}{\partial\tau} + \frac{\partial}{\partial\eta}\big((1-\alpha)V\big) = 0 \tag{14}$$

$$Re\left(\frac{\partial U}{\partial\tau} + V\frac{\partial U}{\partial\eta}\right) = \frac{\partial^2 U}{\partial\eta^2} - \frac{9}{2}\frac{f(\alpha)}{(1-\alpha)}(U-U_{\mathrm{p}}) \tag{15}$$

$$\begin{aligned}
&Re\left(\frac{\partial V}{\partial\tau} + V\frac{\partial V}{\partial\eta}\right) \\
&\quad = \frac{\partial^2 V}{\partial\eta^2} + P - \frac{9}{2}\frac{f(\alpha)}{(1-\alpha)}(V-V_{\mathrm{p}})
\end{aligned} \tag{16}$$

$$\begin{aligned}
&\frac{1}{3}RePr\left(\frac{\partial\theta}{\partial\tau} + V\frac{\partial\theta}{\partial\eta}\right) = \left(\frac{1}{3}+N\right)\frac{\partial^2\theta}{\partial\eta^2} \\
&\quad + \frac{3}{2}(1-\xi)EcPr\frac{f(\alpha)}{(1-\alpha)}\big[(U-U_{\mathrm{p}})^2 + (V-V_{\mathrm{p}})^2\big] \\
&\quad + \frac{1}{3}EcPr\left(\frac{\partial U}{\partial\eta}\right)^2 - \frac{\alpha}{(1-\alpha)}(\theta-\theta_{\mathrm{p}}) + \phi\theta
\end{aligned} \tag{17}$$

$$\frac{\partial\alpha}{\partial\tau} + \frac{\partial}{\partial\eta}(\alpha V_{\mathrm{p}}) = 0 \tag{18}$$

$$\gamma Re\left(\frac{\partial U_{\mathrm{p}}}{\partial\tau} + V_{\mathrm{p}}\frac{\partial U_{\mathrm{p}}}{\partial\eta}\right) = \frac{9}{2}\frac{f(\alpha)}{\alpha}(U-U_{\mathrm{p}}) \tag{19}$$

$$\gamma Re\left(\frac{\partial V_{\mathrm{p}}}{\partial\tau} + V_{\mathrm{p}}\frac{\partial V_{\mathrm{p}}}{\partial\eta}\right) = P - 1 + \frac{9}{2}\frac{f(\alpha)}{\alpha}(V-V_{\mathrm{p}}) \tag{20}$$

$$\begin{aligned}
&\frac{1}{3}RePr\gamma k\left(\frac{\partial\theta_{\mathrm{p}}}{\partial\tau} + V_{\mathrm{p}}\frac{\partial\theta_{\mathrm{p}}}{\partial\eta}\right) \\
&\quad = \frac{3}{2}\xi\frac{f(\alpha)}{\alpha}EcPr\big[(U-U_{\mathrm{p}})^2 + (V-V_{\mathrm{p}})^2\big] \\
&\qquad + (\theta-\theta_{\mathrm{p}})
\end{aligned} \tag{21}$$

where

$$\begin{aligned}
&\gamma = \frac{\rho_{\mathrm{p}}}{\rho}, && Re = \frac{ga^3\gamma}{\nu^2}, && Pr = \frac{\nu}{\kappa} \\
&k = \frac{c_{\mathrm{p}}}{c}, && Ec = \left(\frac{ga^2\gamma}{\nu}\right)^2\frac{1}{c(T_{\mathrm{W}}-T_\infty)} && \\
&\nu = \frac{\mu}{\rho}, && \kappa = \frac{\lambda_{\mathrm{c}}}{\rho c}, && \phi = \frac{1}{3}\frac{Q_0 a^2}{\lambda_{\mathrm{c}}} \\
&N = \frac{16\sigma T_\infty^3}{K\lambda_{\mathrm{c}}} &&&&
\end{aligned} \tag{22}$$

are the particle loading, Reynolds number, Prandtl number, specific heat ratio, Eckert number, kinematic viscosity, the fluid thermal diffusivity, the dimensionless heat generation or absorption coefficient, and the dimensionless thermal radiation coefficient, respectively. ξ $(0 \le \xi \le 1)$ is a dimensionless parameter introduced to apportion the heat dissipation between the phases [18].

According to the orders of magnitude of the dimensionless numbers of the momentum and energy equations given by Apazidis [8], it is concluded that the Eckert numbers for metal particles in gas, water, and oil are approximately 10^{-6}, 10^{-10}, and 10^{-10}, respectively. Therefore, the neglect of the dissipation terms containing Ec in these equations is justified.

Assuming that the volume fraction of particles is constant, equations (14) and (18) give

$$\frac{\partial V}{\partial\eta} = \frac{\partial V_{\mathrm{p}}}{\partial\eta} = 0 \tag{23}$$

Also, with the assumption of zero volumetric flux in the vertical direction as in the case of batch sedimentation [18], one may write

$$\alpha V_{\mathrm{p}} + (1-\alpha)V = 0 \tag{24}$$

Furthermore, assuming that the vertical motion of both phases due to the gravity field has reached its stationary state $(\partial V_{\mathrm{p}}/\partial\tau = \partial V/\partial\tau = 0)$ and using equations (16), (20) and (24) result in the following vertical components of the velocity fields of both phases:

$$V = \frac{2}{9}\frac{\alpha^2(1-\alpha)}{f(\alpha)}, \qquad V_{\mathrm{p}} = -\frac{2}{9}\frac{\alpha(1-\alpha)^2}{f(\alpha)} \tag{25}$$

The interface vertical velocity can be shown to be

$$V_{\mathrm{i}} = \frac{2}{9}\frac{\alpha^2(1-\alpha)^2}{(\alpha_{\mathrm{M}}-\alpha)f(\alpha)} \tag{26}$$

where α_{M} ($\approx$0.6 for spherical particles) is the volume fraction of particles in the dense sediment near the

surface (see [8]). It should be mentioned here that the factor 2/9 in equations (25) and (26) is wrongfully missing from the solutions of Apazidis [9].

The horizontal velocity distributions of both phases (U and U_p) were obtained from the solution of equations (15) and (19) and were reported earlier by Apazidis [8]. Therefore, these solutions will not be repeated herein. The energy equations of both phases can be transformed by using a new coordinate system which moves upwards with the interface velocity V_i such that

$$\eta^* = \eta - V_i \tau \tag{27}$$

to yield

$$\frac{1}{3} Re\,Pr\left[\frac{\partial\theta}{\partial\tau} - (V_i - V)\frac{\partial\theta}{\partial\eta^*}\right] = \left(\frac{1}{3} + N\right)\frac{\partial^2\theta}{\partial\eta^{*2}} - \frac{\alpha}{(1-\alpha)}(\theta - \theta_p) + \phi\theta \tag{28}$$

$$\frac{1}{3} Re\,Pr\,\gamma k\left[\frac{\partial\theta_p}{\partial\tau} - (V_i - V_p)\frac{\partial\theta_p}{\partial\eta^*}\right] = \theta - \theta_p \tag{29}$$

It should be mentioned that if N and ϕ are formally equated to zero, the equations reported by Apazidis [9] will be recovered.

3. ANALYTICAL RESULTS

Analytical solutions for the thermal characteristics of the problem under consideration are obtained for two physical cases. The first case is that of stationary temperature distributions of steady two-phase flow over an isothermal surface while the second case deals with periodic temperature distributions in which the surface is periodically heated.

3.1. Case 1: Stationary temperature distributions

For this case the energy equations of both phases (28) and (29) (with the asterisks being dropped) and the appropriate boundary conditions can be written as

$$-\frac{1}{3} Re\,Pr(V_i - V)\frac{d\theta}{d\eta} = \left(\frac{1}{3} + N\right)\frac{d^2\theta}{d\eta^2} - \frac{\alpha}{(1-\alpha)}(\theta - \theta_p) + \phi\theta \tag{30}$$

$$-\frac{1}{3} Re\,Pr\,\gamma k(V_i - V_p)\frac{d\theta_p}{d\eta} = \theta - \theta_p \tag{31}$$

$$\begin{aligned} &\eta = 0: \quad \theta = 1 \\ &\eta = \infty: \quad \theta = \theta_p = 0 \end{aligned} \tag{32}$$

Equations (32) indicate that the fluid-phase temperature at the wall is uniform and that both the fluid- and particle-phase temperatures far from the surface are equal to the free stream temperature.

Equations (30) and (31) can be combined into a third-order ordinary differential equation in terms of θ_p. This is done by solving for θ from equation (31) and substituting into equation (30) to give

$$B_1\frac{d^3\theta_p}{d\eta^3} + B_2\frac{d^2\theta_p}{d\eta^2} + B_3\frac{d\theta_p}{d\eta} + B_4\theta_p = 0 \tag{33}$$

where

$$\begin{aligned} B_1 &= -\frac{1}{3}\left(\frac{1}{3} + N\right) Re\,Pr\,\gamma k(V_i - V) \\ B_2 &= \left(\frac{1}{3} + N\right) - \frac{1}{9} Re^2 Pr^2 \gamma k(V_i - V)(V_i - V_p) \\ B_3 &= \frac{1}{3}(V_i - V) Re\,Pr + \frac{\alpha Pr\,\gamma k}{3(1-\alpha)}(V_i - V) \\ &\quad - \frac{1}{3} Re\,Pr(V_i - V_p)\phi \\ B_4 &= \phi \end{aligned} \tag{34}$$

The physical solution of equation (33) requires that the characteristic equation

$$B_1 r^3 + B_2 r^2 + B_3 r + B_4 = 0 \tag{35}$$

($\theta_p = C\exp(r\eta)$, C is a constant) had two positive real roots and one negative real root. More than one negative root makes the problem to be underdetermined. While there is no analytical method to show the existence of two positive and one negative roots for equation (35), this condition was satisfied in all the results obtained for this case. Therefore, the solution for θ_p can be written as

$$\theta_p(\eta) = C_1\exp(-r_1\eta) + C_2\exp(-r_2\eta) + C_3\exp(-r_3\eta) \qquad r_1, r_2, r_3 > 0 \tag{36}$$

where C_1, C_2 and C_3 are arbitrary constants to be found by the application of the boundary conditions.

Application of equations (32) produces

$$\begin{aligned} C_1 &= \frac{1}{1 + r_1(\frac{1}{3} Re\,Pr\,\gamma k)(V_i - V_p)} \\ C_2 &= 0, \qquad C_3 = 0 \end{aligned} \tag{37}$$

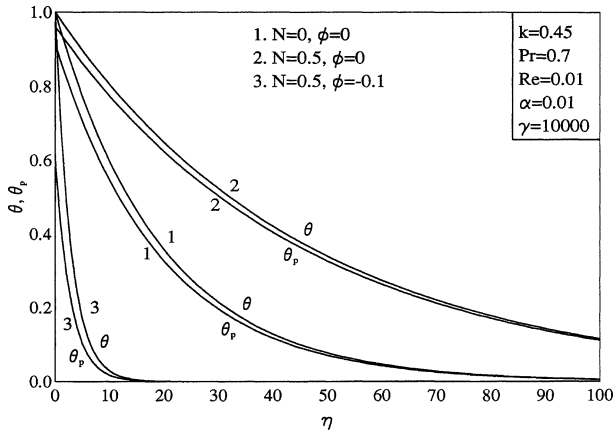

Figure 1. Effects of N and ϕ on θ and θ_p for air–metal particles.

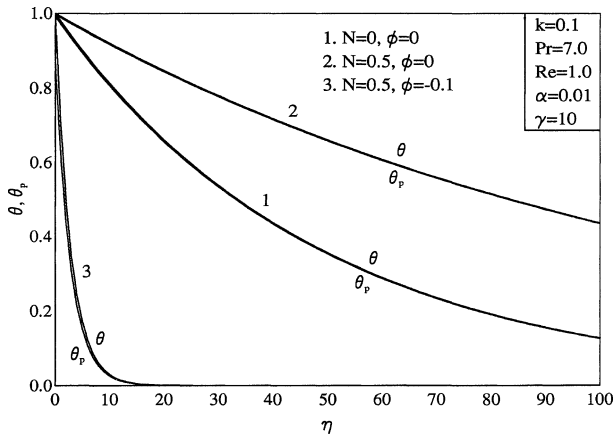

Figure 2. Effects of N and ϕ on θ and θ_p for water–metal particles.

The corresponding solution for $\theta(\eta)$ can then be written as

$$\theta(\eta) = \exp(-r_1\eta) \tag{38}$$

Figures 1–3 depict the influence of the thermal radiation coefficient N and the heat absorption coefficient ϕ on the fluid-phase temperature θ and the particle-phase temperature θ_p for suspensions of air–metal particles, water–metal particles, and oil–metal particles, respectively. The values of the physical parameters employed to produce these and all subsequent figures represent actual values for the fluid–particle combinations considered (see [9]). The obvious temperature lag of the particle phase compared to the fluid phase is apparent in these figures. Physically speaking, fluid-phase heat absorption effects have the tendency to decrease the fluid-phase temperature. As a result and through the interphase

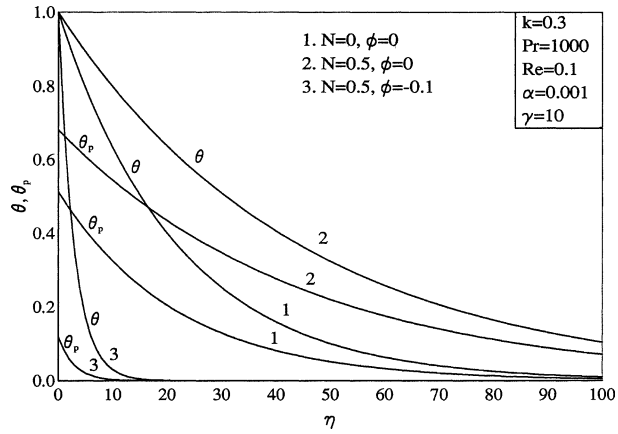

Figure 3. Effects of N and ϕ on θ and θ_p for oil–metal particles.

heat transfer, the temperature of the particle phase decreases. This is clearly shown in *figures 1–3*. On the other hand, increases in the thermal radiation coefficient N enhances the thermal diffusion of the fluid phase causing its temperature to increase. Consequently, and as mentioned before, the particle-phase temperature increases. The thermal layers of both phases are observed to increase as N increases and decreases as ϕ decreases for all mixture types considered herein. *Figures 1–3* are selected to show different levels of temperature deficit between the phases by proper choice of the Reynolds number *Re* and the particle volume fraction α. *Figure 1* for air–metal particles flow shows a moderate temperature deficit between the phases while *figure 2* for water–metal particles flow shows small temperature deficit and *figure 3* for oil–metal particles flow displays large particle-phase temperature lag compared to the fluid phase. In the absence of heat absorption and thermal radiation ($\phi = 0$, $N = 0$) and without the factor 2/9 in the results of V, V_p and V_i, the above solutions are in excellent agreement with the results reported by Apazidis [9]. It should be noted that no physically-correct solutions were possible for positive values of ϕ (heat generation).

3.2. Case 2: Periodic temperature distributions

For this case the fluid-phase wall temperature has the dimensional form

$$T_w = T_\infty + (T_w - T_\infty)\cos(\omega t) \tag{39}$$

where ω is the frequency of wall temperature oscillation. In dimensionless form, the wall temperature becomes

$$\theta(\tau, 0) = \cos(\omega\tau) \tag{40}$$

The thermal equilibrium of both phases in the free stream is represented by

$$\theta(\tau, \infty) = \theta_p(\tau, \infty) = 0 \tag{41}$$

The general unsteady equations (28) and (29) are solved subject to equations (40) and (41) for $\theta(\tau, \eta)$ and $\theta_p(\tau, \eta)$ by assuming

$$\theta(\tau, \eta) = \cos(\omega\tau + \beta\eta)\exp(-s\eta) \tag{42}$$

$$\theta_p(\tau, \eta) = \left[D_1\cos(\omega\tau + \beta\eta) + D_2\sin(\omega\tau + \beta\eta)\right] \cdot \exp(-s\eta) \tag{43}$$

where β, D_1, D_2 and s are constants which make equations (28) and (29) subject to equations (40) and (41) identically satisfied by the solutions (42) and (43).

Substitution of equations (42) and (43) into equations (28) and (29) results in two equations of the general form

$$P_1\cos(\omega\tau + \beta\eta) + P_2\sin(\omega\tau + \beta\eta) = 0 \tag{44}$$

where P_1 and P_2 are functions of the constants β, D_1, D_2 and s. Equating P_1 and P_2 of each of the obtained two equations results in the following system of equations:

$$\frac{1}{3}RePr\,\gamma k\left[D_2\omega - (V_i - V_p)(D_2\beta - sD_1)\right] + D_1 - 1 = 0 \tag{45}$$

$$-\frac{1}{3}RePr\,\gamma k\left[D_1\omega - (V_i - V_p)(D_1\beta + sD_2)\right] + D_2 = 0 \tag{46}$$

$$\frac{1}{3}RePr(V_i - V)s + \left(\frac{1}{3} + N\right)(\beta^2 - s^2) + \frac{\alpha}{(1-\alpha)}(1 - D_1) - \phi = 0 \tag{47}$$

$$-\frac{1}{3}RePr\left[\omega - (V_i - V)\beta\right] - \left(\frac{1}{3} + N\right)(2\beta s) - \frac{\alpha}{(1-\alpha)}D_2 = 0 \tag{48}$$

Equations (45)–(48) represent four nonlinear equations with four unknowns (β, D_1, D_2 and s) which must be solved numerically. For fast convergence of the solutions, the following procedure is followed. First, equations (47) and (48) are solved for D_1 and D_2 in terms of β and s, respectively. Secondly, the obtained expressions for D_1 and D_2 are then substituted into equation (46) which produces a quadratic equation in s with the coefficients containing the constant β. For an assumed value of β and given values of the involved parameters, the roots of this quadratic equation which are real and of opposite signs can be obtained. Therefore, the negative root is chosen and its absolute value is the needed value of s. With the value of s being known for the assumed β, the constants D_1 and D_2 can then be determined from equations (47) and (48) as mentioned above. Finally, the values of s, D_1 and D_2 are substituted into equation (45) which is then solved for β. As long as $\beta_{assumed} \neq \beta_{obtained}$, the same iteration procedure continues until convergence is obtained. Results based on the solutions of θ and θ_p given by equations (42) and (43) are displayed in *figures 4–8*.

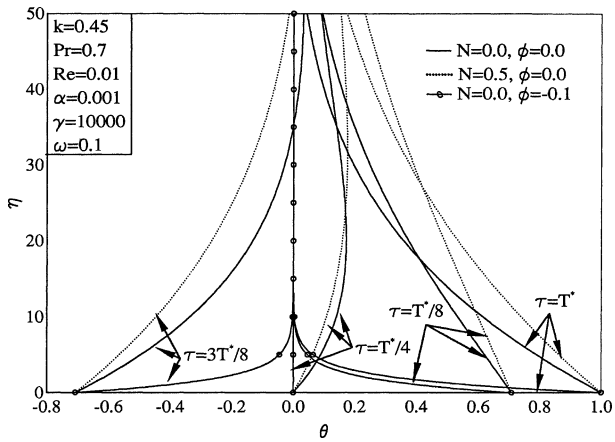

Figure 4. Effects of N and ϕ on periodic fluid-phase temperature distribution in air–particle flow.

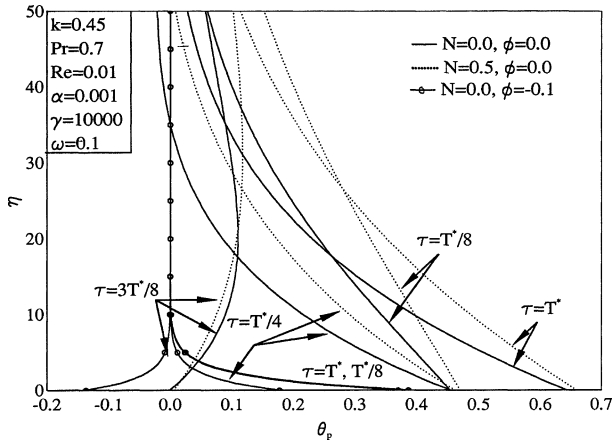

Figure 5. Effects of N and ϕ on periodic particle-phase temperature distribution in air–particle flow.

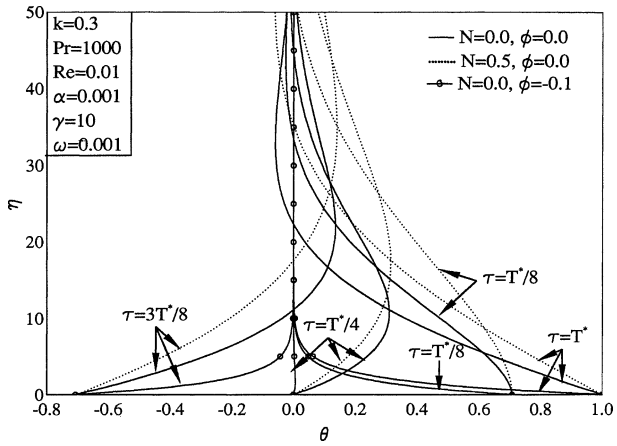

Figure 6. Effects of N and ϕ on periodic fluid-phase temperature distribution in oil–particle flow.

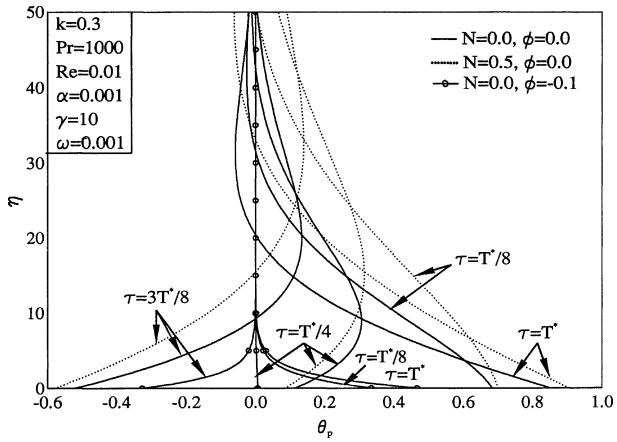

Figure 7. Effects of N and ϕ on periodic particle-phase temperature in oil–particle flow.

Figures 4 and *5* display the effects of the thermal radiation coefficient N and heat absorption coefficient ϕ on the fluid- and particle-phase periodic temperature distributions in air–particle flow for $Re = 0.01$ and $\alpha = 0.001$, respectively. As in the stationary case, thermal radiation increases both the fluid- and particle-phase temperatures (for $\tau = T^*$ and $\tau = T^*/8$) while heat absorption produces lower temperature distributions for both phases (for $\tau = T^*$ and $\tau = T^*/8$). Also, large temperature differences between the phases are obtained at high values of the relative velocity and large relaxation times for energy transfer. Thus, it is expected that large temperature differences occur for air–particle mixtures with low particle concentrations and at high Reynolds numbers due to high interphase drag as illustrated in *figures 4* and *5*. It is also observed from these figures that

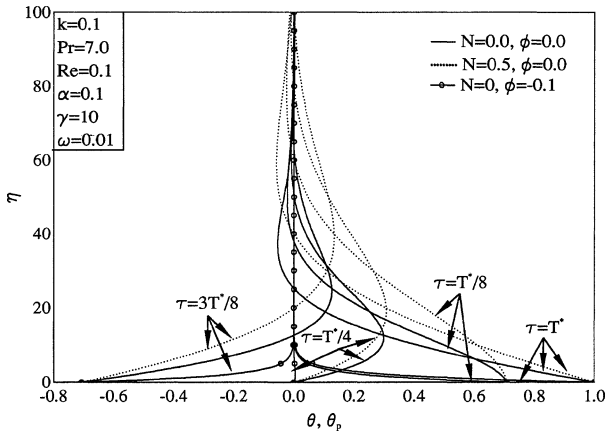

Figure 8. Effects of N and ϕ on periodic temperature distributions in water–particle flow.

the heat absorption effect speeds up the approach of both phases to the free stream thermal conditions.

In *figures 6* and *7*, similar plots for the fluid-phase temperature θ and the particle-phase temperature θ_p as in *figures 4* and *5* but for an oil–particle mixture with $Re = 0.01$ and $\alpha = 0.001$. Due to the large value of Prandtl number for this case, large temperature differences between the phases occur. The effects of N and ϕ on θ and θ_p are the same as in *figures 4* and *5*.

Plots for θ and θ_p for a water–particle mixture with $Re = 0.1$ and $\alpha = 0.1$ are presented in *figure 8*. It is observed that both phases are in thermal equilibrium. This is due to insignificant interphase drag and small thermal relaxation times. These behaviours are consistent with those reported earlier by Apazidis [9]. Again, in the absence of heat absorption ($\phi = 0$) and thermal radiation ($N = 0$), the results of Apazidis [9] are obtained provided that the factor $2/9$ in the expressions of V, V_p and V_i is absent.

Of special interest for this problem is the rate of heat transfer between the sediment layer on the surface and the suspension above it. The total heat transfer rate (without the radiative heat transfer part) through the moving interface between the sediment and the suspension is the sum of the convective heat transfer rate of the fluid phase and the sensible heat transfer of the particles. This is given by

$$q_T = q_f + q_p \tag{49}$$

where

$$q_f = -(1-\alpha)\lambda_c \left.\frac{\partial T}{\partial y}\right|_{y=0} = -(1-\alpha)\frac{\lambda_c}{a}(T_w - T_\infty)\left.\frac{\partial \theta}{\partial \eta}\right|_{\eta=0} \tag{50}$$

$$q_p = \alpha c_p \rho_p (v_p - v)(T_p - T_w)\big|_{\eta=0}$$
$$= \alpha c_p \rho_p \frac{ga^2\gamma}{\nu}(T_w - T_\infty)(V_p - V_i)(\theta_p - 1)\big|_{\eta=0} \quad (51)$$

The dimensionless form of equation (49) can be written as

$$Q_T = Q_f + Q_p \quad (52)$$

where

$$Q_f = -(1-\alpha)\frac{\partial\theta}{\partial\eta}\bigg|_{\eta=0}$$
$$Q_p = \alpha\, Re\, Pr\, \gamma k (V_p - V_i)(\theta_p - 1)\big|_{\eta=0} \quad (53)$$

and Q_T is nondimensionized by $\kappa\rho c(T_w - T_\infty)/a$.

For the case of stationary temperature distributions, equations (53) are given by

$$Q_f = (1-\alpha)r_1$$
$$Q_p = \alpha\, Re\, Pr\, \gamma k (V_p - V_i) \cdot \left[\frac{1}{1 - \frac{1}{3}\alpha\, Re\, Pr\, \gamma k (V_p - V_i)} - 1\right] \quad (54)$$

Figures 9 and *10* illustrate the influence of the thermal radiation coefficient N and the heat absorption coefficient ϕ on the dimensionless fluid-phase heat transfer rate Q_f, dimensionless particle-phase heat transfer rate Q_p, and the dimensionless total heat transfer rate Q_T for an air–metal particles suspension at different particle-phase volume fraction levels, respectively. The heat transfer contribution of each of the phases is dependent of the value of the Reynolds number *Re*. For small *Re* values, as considered in *figures 9* and *10*, most of the heat transfer contribution is due to the convective heat transfer of the fluid phase. It is seen from *figure 1* that the wall slope of the fluid-phase temperature increases as N increases. This causes the rate of heat transfer of the fluid phase to decrease at any value of the particle volume fraction α. In the same way, the wall particle-phase temperature increases as N increases. This produces lower sensible heat transfer rates of the particles for all values of α. These behaviors are depicted clearly in *figure 9*. On the other hand, both the wall slope of the fluid-phase temperature and the wall particle-phase temperature decrease as the heat absorption coefficient ϕ decreases. This has the direct effect of increasing the rates of convective fluid-phase heat transfer, the sensible particle-phase heat transfer, and the total heat flux as shown in *figure 10*.

Figures 11–14 display the influence of N and ϕ on Q_f, Q_p and Q_T for water–metal particles and oil–metal particles suspensions. In these figures, the same effect

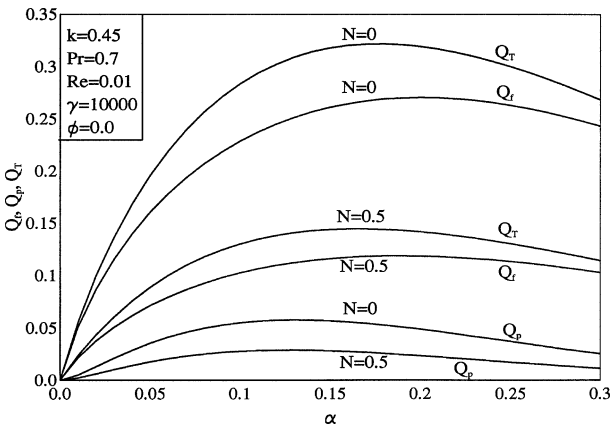

Figure 9. Effects of α and N on heat fluxes in air–particle flow.

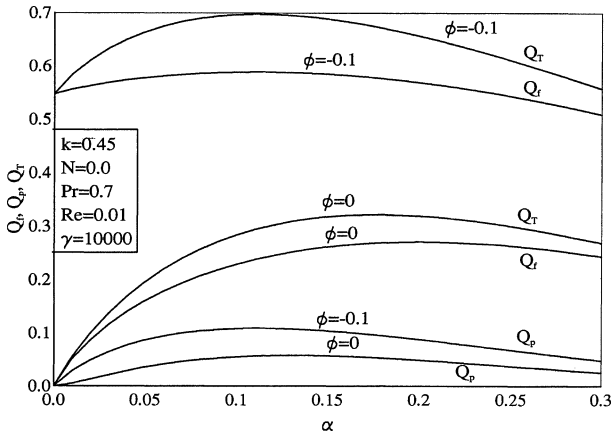

Figure 10. Effects of α and ϕ on heat fluxes in air–particle flow.

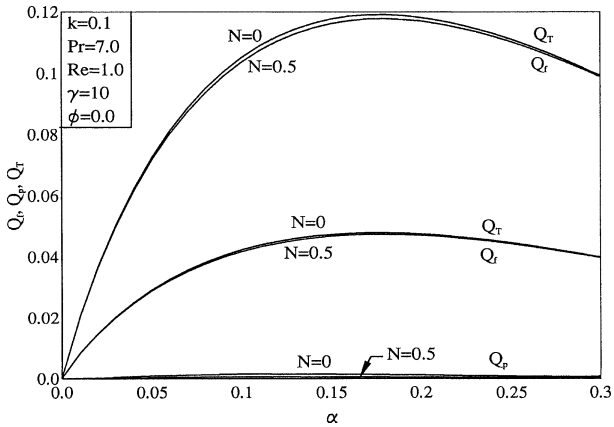

Figure 11. Effects of α and N on heat fluxes in water–particle flow.

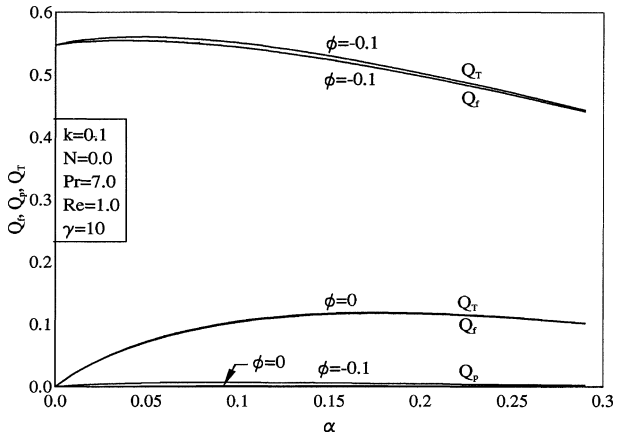

Figure 12. Effects of α and ϕ on heat fluxes in water–particle flow.

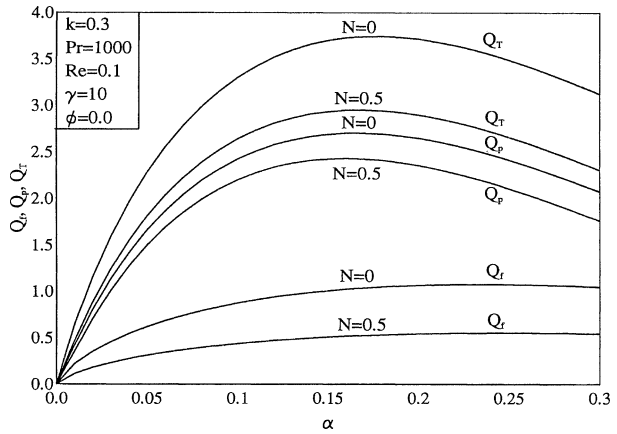

Figure 13. Effects of α and N on heat fluxes in oil–particle flow.

of N and ϕ on Q_f, Q_p and Q_T are observed for these suspensions as discussed earlier for air–metal particles suspensions. The distinct behavior in these figures is that for a water–particle suspension at $Re = 1$, the total heat transfer is almost entirely due to the convective heat transfer of the fluid phase while for an oil–particle suspension at $Re = 0.1$, the sensible heat transfer of the particles is more predominant than that of the fluid phase. It should be noted that in *figures 9–14* the total heat transfer rate shows an increasing behavior with increases in the particulate volume fraction α up to a certain value of α and then it decreases beyond this value. Physically, when the sensible heat transfer of the particles is dominant, increasing the volume fraction of particles α increases the total heat transfer rate. Also, increases in the values of α have the tendency to increase the coupling between the phases which causes decreases in both the relative velocity and temperature

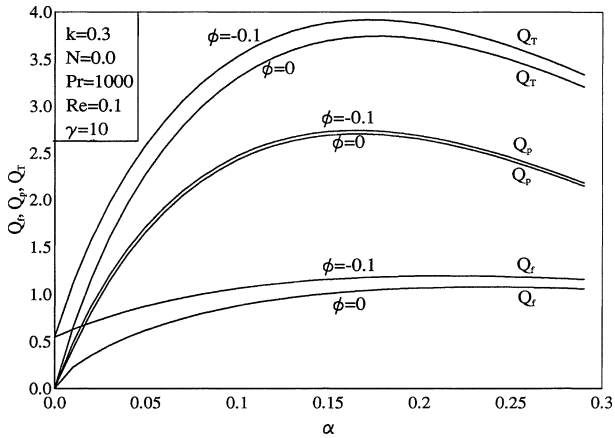

Figure 14. Effects of α and ϕ on heat fluxes in oil–particle flow.

between the particles and the interface. However, at a certain value of α, the effect of reduction of the relative velocity and temperature becomes greater than the effect of increase of α on Q_T. This causes Q_T to decrease. Furthermore, when the convective heat transfer of the fluid phase is dominant, initial increases in α produce higher fluid-phase temperature gradients at the interface causing higher heat transfer rates. However, as α is increased further, both the relative velocity and temperature decreases causing lower fluid-phase temperature gradients at the interface. This causes the convective heat transfer rate and, therefore, the total heat flux to decrease.

4. CONCLUSION

This paper focused on the study of the effects of fluid-phase heat generation or absorption and thermal radiation on the problem of heat transfer in a particulate suspension flow past a horizontal heated surface in the presence of a gravity field. Analytical solutions for the temperature distributions and heat fluxes of both phases were obtained for stationary and periodic thermal wall conditions. The study was done on suspensions of metal particles in air, water, and oil. It was found that the temperatures as well as the thermal wall layers of both the fluid and the particle phases increased due to the presence of thermal radiation and decreased owing the presence of heat absorption effects. As a result, the thermal radiation effect decreased the total rate of heat transfer for all mixtures considered while the heat absorption effect enhanced the total heat flux. In general, the total heat flux increased with increasing values of the particulate

volume fraction to a maximum after which it showed a decreasing behavior. Larger temperature deficit between the phases were found at high density ratios between the phases, high Prandtl numbers, and high Reynolds numbers.

REFERENCES

[1] Yiantsios S.G., Karabelas A.J., The effect of gravity on the deposition of micron-sized particles on smooth surfaces, Int. J. Multiphase Flow 24 (1998) 283–293.

[2] Jia X., Williams R.A., Particle deposition at a charged solid/liquid interface, Chem. Engrg. Comm. 91 (1990) 127–198.

[3] Van de Ven T.G.M., Colloidal Hydrodynamics, Academic Press, London, 1989.

[4] Yao K.M., Habibian M.T., O'Melia C.R., Water and waste water filtration: concepts and applications, Env. Sci. Techn. 5 (1971) 1105–1112.

[5] Adamczyk Z., van de Ven T.G.M., Deposition of particles under external forces in laminar flow through parallel-plate and cylindrical channels, J. Colloid Interface Sci. 80 (1981) 340–356.

[6] Adamczyk Z., van de Ven T.G.M., Particle transfer to a plate in uniform flow, Chem. Engrg. Sci. 37 (1982) 869–880.

[7] Marmur A., Ruckenstein E., Gravity and cell adhesion, J. Colloid Interface Sci. 114 (1986) 261–266.

[8] Apazidis N., On two-dimensional laminar flows of a particulate suspension in the presence of a gravity field, Int. J. Multiphase Flow 11 (1985) 657–698.

[9] Apazidis N., Temperature distribution and heat transfer in a particle–fluid flow past a heated horizontal plate, Int. J. Multiphase Flow 16 (1990) 495–513.

[10] Dahlkild A.A., The motion of Brownian particles and sediment on an inclined plate, J. Fluid Mech. 337 (1997) 25–47.

[11] Vajravelu K., Nayfeh J., Hydromagnetic convection at a cone and a wedge, Int. Commun. Heat Mass Tran. 19 (1992) 701–710.

[12] Vajravelu K., Hadjinicolaou A., Heat transfer in a viscous fluid over a stretching sheet with viscous dissipation and internal heat generation, Int. Commun. Heat Mass Tran. 20 (1993) 417–430.

[13] Raptis A., Flow of a micropolar fluid past a continuously moving plate by the presence of radiation, J. Heat Mass Tran. 41 (1998) 2865–2866.

[14] Raptis A., Radiation and free convection flow through a porous medium, Int. Commun. Heat Mass Tran. 25 (1998) 289–295.

[15] Tien C.L., Vafai K., Convective and radiative heat transfer in porous media, Advances in Applied Mechanics 27 (1990) 225–281.

[16] Vortmeyer D., Radiation in packed solids, in: Proceedings of the 6th International Heat Transfer Conference, Vol. 6, 1978, pp. 525–539.

[17] Tien C.L., Radiation properties of particulates, in: Handbook of Heat Transfer Fundamentals, 2nd Edition, Hemisphere, New York, 1985, pp. 14.83–14.91.

[18] Wallis G.B., One-dimensional Two-phase Flow, MaGraw-Hill, New York, 1969.

[19] Kynch G.J., A theory of sedimentation, Trans. Faraday Soc. 48 (1952) 166–176.

[20] Marble F.E., Dynamics of dusty gases, Annual Review of Fluid Mechanics 2 (1970) 397–446.

[21] Tam K.W., The drag on a cloud of spherical particles in low Reynolds number flow, J. Fluid Mech. 38 (1969) 537–546.